MODELING OF OCEANIC GAS HYDRATE INSTABILITY AND METHANE RELEASE IN RESPONSE TO CLIMATE CHANGE

Matthew T. Reagan*
George J. Moridis

Earth Sciences Division
Lawrence Berkeley National Laboratory
1 Cyclotron Rd., Berkeley, CA 94720
USA

ABSTRACT

Paleooceanographic evidence has been used to postulate that methane from oceanic hydrates may have had a significant role in regulating global climate, implicating global oceanic deposits of methane gas hydrate as the main culprit in instances of rapid climate change that have occurred in the past. However, the behavior of contemporary oceanic methane hydrate deposits subjected to rapid temperature changes, like those predicted under future climate change scenarios, is poorly understood. To determine the fate of the carbon stored in these hydrates, we performed simulations of oceanic gas hydrate accumulations subjected to temperature changes at the seafloor and assessed the potential for methane release into the ocean. Our modeling analysis considered the properties of benthic sediments, the saturation and distribution of the hydrates, the ocean depth, the initial seafloor temperature, and for the first time, estimated the effect of benthic biogeochemical activity. The results show that shallow deposits—such as those found in arctic regions or in the Gulf of Mexico—can undergo rapid dissociation and produce significant methane fluxes of 2 to 13 mol/yr/m^2 over a period of decades, and release up to 1,100 mol of methane per m^2 of seafloor in a century. These fluxes may exceed the ability of the seafloor environment (via anaerobic oxidation of methane) to consume the released methane or sequester the carbon. These results will provide a source term to regional or global climate models in order to assess the coupling of gas hydrate deposits to changes in the global climate.

Keywords: gas hydrates, climate change

NOMENCLATURE

T	temperature [˚C]
P	pressure [bar]
S_H	hydrate saturation
S_G	gas saturation
k	permeability [m^2]
ϕ	porosity
Q_M	methane flux at the seafloor [mol/yr/m^3]
V_{aq}	aqueous flow velocity at seafloor [cm/yr]
X_M	aqueous methane concentration [mM]
C_M	cumulative methane release [mol/m^3]
STP	standard temperature and pressure

INTRODUCTION

Gas hydrates are solid crystalline compounds in which gas molecules are lodged within the lattices of water clathrate crystals [1]. Natural gas hydrate deposits occur in two distinctly different geologic settings where the necessary low temperatures and high pressures exist for their formation and stability: in the permafrost and in deep ocean sediments. A review of existing literature indicates that estimates of in situ methane hydrate reserves are enormous, ranging between 10^{15} m^3 STP [2] to as high as 7.6×10^{18} m^3 STP [3]. Many investigators have attempted to assess the total amount of methane hydrate currently residing in the deep ocean and along continental margins. These estimates began an initial "consensus value" of 10,000 Gt through work by various investigators [4-7]. More recently, Milkov [2] proposed a total of 500-2,500 Gt of methane-

* Corresponding author: Phone: +1 510 486 6517 Fax +1 510 486 5686 E-mail: mtreagan@lbl.gov

derived carbon (1-5 x 10^{15} m^3 STP). Two of the most recent studies, each accounting for the coupled contribution of organic matter decomposition and mass transport, have produced drastically different results. Klauda and Sandler [8] provide an upper estimate of 74,400 Gt of methane carbon in hydrate form (27,300 Gt along continental margins, while Buffett and Archer [9] used both compaction and advection in a 1-D methanogenesis/hydrate formation model to reach an estimate of 3,000 Gt of methane in hydrate and 2,000 Gt of gaseous methane existing in a stable state under current climate conditions.

In oceanic deposits, the range of depth over which hydrates remain stable (the gas hydrate stability zone, GHSZ) depends on the pressure *P* (imposed by the water depth) and temperature *T*. The GHSZ may extend upward to 300 m - 400 m depths [10]. A pressure decrease due to lowering of the sea level, or an increase in the temperature of the ocean water in contact with the seabed, could induce hydrate dissociation and lead to the formation of gas. Shallow deposits are more prone to destabilization due to their proximity to the edge of the GHSZ and the shorter time needed for temperature changes to propagate into the deposit. Shallow deposits may also be at greater risk for destabilization than estimated by broad global surveys. The Gulf of Mexico, in particular, may contain up to 500 Gt of methane-derived carbon as hydrates in its sediments [11] and hundreds of Gt of methane are expected to exist within Arctic Ocean sediments [12].

An increase in the temperature of the ocean water at the seafloor could induce hydrate dissociation and lead to methane release. The released CH_4 could be added to the global carbon reservoir by ebullition or diffusion into the water column, advection by ocean currents, chemical and biochemical activity in the water column, and finally by ebullition into the atmosphere if the rate of CH_4 release were to exceed the rate of oxidation [13]. Such a release could have potentially dramatic climatic consequences because it could lead to a sequence of cascading effects, involving amplified atmospheric and oceanic warming and accelerated dissociation of the remaining hydrates. Recent deep ocean surveys have found pockmarks and other structures that indicate large fluid releases at the seafloor in the past [14] and hydrate dissociation and gas release is a either a possible cause or consequence of submarine slope failure and landslides [15]. Computational studies that coupled a simplified global clathrate reservoir to a time-dependent ocean carbon cycle model [16] showed a significant contribution to climate change on millennial timescales. Recent simulations of hydrate dissociation in response to ocean temperature changes [17] indicated that shallow systems can release significant quantities of methane on decadal timescales when subjected to as little as 1 ^oC of warming applied at the top of hydrate-bearing sediments (HBS). In contrast, simulations of the behavior of cold, deep-sea hydrates [17, 18] do not indicate widespread instability or methane release.

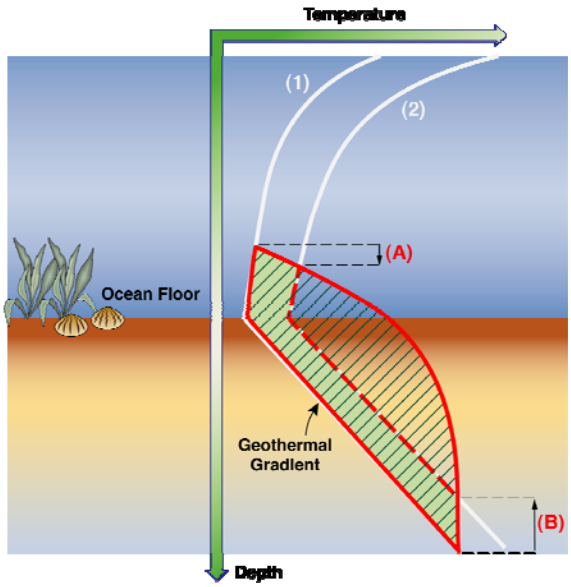

Figure 1: Schematic of the GHSZ in the seafloor environment (not to scale).

The process of dissociation and release is illustrated schematically in Figure 1. An increase in ocean water temperature at the seafloor, from temperature profile (1) to profile (2), lowers the top of the GHSZ (A) and raises the bottom of the GHSZ (B), and as such, the temperature profile intersects a reduced region of the hydrate stability curve (red-bounded area). In this illustration, hydrate existing in the sediments at depth (B) is destabilized and may dissociate. In nature, the GHSZ may extend above the seafloor (as shown), or the top of the GHSZ may lie at or below the seafloor. In addition, the process of hydrate dissociation is regulated by multiple factors, including flow of heat from below the hydrate

deposit, fluid flow induced by hydrate dissociation, the thermal properties of the sediments (regulating the propagation of temperature changes into the sediment column), and the enthalpy of dissociation of the hydrates themselves. The coupled thermodynamic, hydrologic, and transport processes that occur with ocean sediments are considered in the following computational study.

An additional layer exists between hydrate stability in ocean sediments and carbon cycles in the oceans and atmosphere. The benthic sediment environment, from the seafloor down to several meters into the sediment column, is biologically active and home to a complex network of chemosynthetic communities, bacteria, and archaea, which may play a role in the interaction between methane derived from hydrates and the global biosphere [19, 20].

The sum of all processes acting on sediments in an aqueous environment is known as diagenesis. Extensive simulation work [21, 22] has examined benthic sediment chemistry with respect to degradation of organic matter into methane, and the interaction of methane with oxygen and dissolved minerals within pore waters. Luff and collaborators [23, 24] modeled fluid flow, biogeochemistry, and carbonate precipitation at a 775 m-deep cold vent site at Hydrate Ridge on the Cascadia margin. Biologically mediated oxidation of the rising methane by sulfate (anaerobic oxidation of methane, AOM) occurs in a narrow zone at the top of the sediment column, releasing sulfide and bicarbonate into the pore water:

$$CH_4 + SO_4^{2-} \rightarrow HCO_3^- + HS^- + H_2O \qquad (1)$$

Aerobic bacteria at the sediment surface may then oxidize the sulfide with available dissolved oxygen, and the bicarbonate increases pH and encourages precipitation (and perhaps sequestration) of the carbon as solid carbonate:

$$Ca^{2+} + 2HCO_3^- \Leftrightarrow CaCO_3(s) + CO_2 + H_2O \qquad (2)$$

With respect to rapid or chronic hydrate decomposition and methane release, biogeochemical reactions may have the potential to convert (to CO_2 or bicarbonate alkalinity) or sequester (as solid carbonate) some or much of the methane released in climate warming scenarios [25].

Methane that reaches the seafloor in gaseous form may also escape in the form of bubbles. Once exposed to the environment of the open water column, methane is subject to conventional aerobic oxidation [26], or it may be transported though the upper region of the ocean, where atmospheric ventilation times are short compared to oxidation rates [27].

MODELS AND METHODS

Simulation tools

The TOUGH+HYDRATE code [28] describes multiphase flow and transport in hydrate-bearing geologic media. It includes complete, coupled mass and energy transport within porous media, and also describes the full phase behavior of water, methane, solid hydrate, ice, and inhibitor species [29]. The code, validated in laboratory experiments [30] and field studies [31], was recently used in preliminary studies of hydrate dissociation in oceanic sediments [17] and this work is a continuation of that research.

Used as a diagenetic numerical model, C.CANDI [22] is a specialized reactive transport code developed from the earlier diagenesis models of Boudreau [21]. The model describes 1-D aqueous flow in porous media and the transport and reaction of up to 29 chemical species. The chemical component includes 6 primary and 17 secondary redox reactions, recognizes 4 acid/base equilibria, quantifies the precipitation/dissolution of minerals, and can be used to calculate equilibrium or non-steady-state concentration profiles at fine (< 0.1 cm) resolution. We use the stand-alone C.CANDI application interactively to assess, for the first time, the potential reactive transport consequences of climate-change-induced methane releases.

Setup of 1-D HBS system

We simulate two types of hydrate accumulations representing disperse, low-saturation deposits with an initial hydrate saturation, S_H, of 0.03 [32] reflecting the high end of the estimated global average saturation [12] for stratigraphic deposits.

Case I: The first case involves a shallow, warmer hydrate deposit at 570 m depth, $T_{i,s}$ = 6 ^{o}C, and a geothermal gradient of 2.8 ˚C/100m. This case is

representative of Gulf of Mexico deposits [33], with the top of the GHSZ just above the seafloor, a scenario where seafloor hydrates have been observed in-situ.

Case II. The second case describes shallow, cold hydrate deposits at 320 m depth, $T_{i,s}$ = 0.4 °C, geothermal gradient of 3 °C/100m, representative of conditions on the arctic continental shelf, with the top of the GHSZ located at the seafloor.

The representation of each case in this study involves a vertical, 1-D domain describing the sediment column from the seafloor downward. The initial condition includes a hydrostatic pressure distribution, a constant geothermal gradient, and uniform hydrate saturation in the sediment column from the seafloor to the bottom of the GHSZ. Physical parameters for the sediments are listed in Table 1. The intrinsic permeability, $k = 10^{-15}$ m^2 (1 mD), is within the reported range of oceanic sediments [34, 35] and represents the more common stratigraphic deposits [2, 32], in contrast to the less common, more permeable, and often more saturated structural deposits near sites of active methane seepage and/or venting. The porosity $\varphi = 0.3$ is typical for unconsolidated marine sediments near the mudline [34].

Constant pressure (corresponding to a constant water depth and salinity) is maintained at the top of the sediment column, while the temperature at the top boundary, representing the water at the ocean floor, is varied. The top of the sediment column allows heat and mass transfer between the sediment column and the bulk ocean. The sediment column is modeled to a depth of 360 m below the seafloor, well beyond the reach of temperature propagation over the simulated time period. The entire column is initially equilibrated to steady-state conditions (P and T) to ensure stable temperature and pressure gradients and to establish the location and extent of the GHSZ.

Results from recent simulations coupling ocean circulation, atmospheric circulation, and atmospheric chemistry [36] suggest that, under current climate conditions and a 1%/yr increase in atmospheric CO_2, the temperature at the seafloor would rise by 1 °C over the next 100 yr, and possibly by another 3 °C in the following century. Consequently, we choose simple linear temperature increases of ΔT = 1, 3, and 5 °C over a 100 yr period at the upper boundary of the simulated domain to describe the evolution of ocean temperature at the seafloor. We record methane fluxes and fluid flow velocities at the seafloor. These cases, although rough schematics of the wide range of possible hydrate depths, distributions, and saturations, allow a systematic examination of the many coupled processes that drive and regulate hydrate dissociation.

Parameter	Value
Initial salt mass fraction in the ocean and pore water X_0	0.035
Gas composition	100% CH_4
Permeability, k	10^{-15} m^2 (1 mD)
Porosity, ϕ	0.30
Dry thermal conductivity, k_{Sd}	1.0 W/m/K
Wet thermal conductivity, k_{Sw}	3.3 W/m/K
Composite thermal conductivity k_Θ model [37]	$k_\Theta = (\sqrt{S_H} + \sqrt{S_A}) \cdot (k_{Sw} - k_{Sd}) + k_{Sd}$
Capillary pressure model [38]	$P_{cap} = -P_0 \left[(S^*)^{-1/\lambda} - 1 \right]^{\lambda}$ $S^* = \frac{(S_A - S_{irA})}{(S_{mxA} - S_{irA})}$
S_{irA}	0.19
P_0	2000 Pa
λ	0.45
Relative permeability model, Modified Stone [39]	$k_{rA} = (S_A^*)^n$ $k_{rG} = (S_G^*)^n$ $S_A^* = (S_A - S_{irA})/(1 - S_{irA})$ $S_G^* = (S_G - S_{irG})/(1 - S_{irA})$
n	4
S_{irG}	0.02
S_{irA}	0.20

Table 1: Physical properties parameters for the hydrate-bearing sediment system simulated with TOUGH+HYDRATE.

RESULTS

Release rates

Fluxes of methane, as measured at the top of the sediment column, are shown in Figure 2. This is a combined flux of methane in gas and aqueous phases, measured for all three simulated linear temperature variations—1, 3, and 5 °C/100 yr.—plotted vs. time for Case I and Case II. Most notable is the near-order-of-magnitude difference between the instantaneous methane fluxes in the two cases, despite identical initial hydrate saturations and parallel temperature change scenarios.

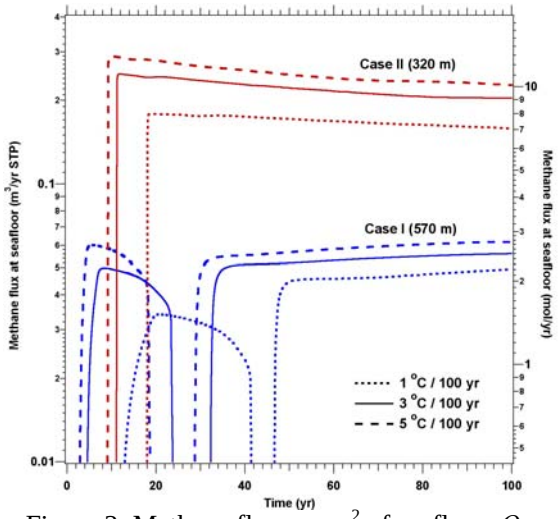

Figure 2: Methane flux per m^2 of seafloor, Q_M, for Case I and Case II undergoing 1, 3, and 5 °C temperature increases.

For Case I, as previously reported [17], the total flux, Q_M, exhibits an initial peak, describing the transport of dissolved methane transported in the aqueous phase, followed by a second surge of methane, primarily in the gaseous phase. The lag between the beginning of dissociation and the arrival of mobile, buoyant gaseous methane at the seafloor reflects the evolution and expansion of gas formed during the initial dissociation driving methane-saturated fluids away from the dissociation zone. The magnitude of the temperature change (and equally, the rate of temperature increase) affects the rate of dissociation, as seen in both 1) decreased instantaneous methane fluxes under more gradual change, and 2) a delay in the arrival of aqueous methane flux and the arrival of the gaseous methane plume. The seafloor fluxes range from Q_M = 2.2 to 2.8 mol CH_4/yr (0.049 to 0.062 m^3 CH_4/yr at standard temperature and pressure, STP) per m^2 of seafloor. Aqueous flow velocities, V_{aq}, at the top of the sediment column peak at 4.3 to 7.6 cm/yr.

For Case II (320 m depth, 0.4 °C initial temperature) the arrival of the methane is delayed for all cases. For each temperature change scenario, the peak instantaneous methane flux is up to 5 times greater than the peak flux in Case I. In this case, released methane in both the aqueous and gas phases arrives at the seafloor at roughly the same time, quickly reaches peak flux, which is then maintained (and near-constant) throughout the 100 yr simulation timeframe. Peak fluxes range from Q_M = 8.0 mol/yr (0.18 m^3/yr STP) to Q_M = 13 mol/yr (0.3 m^3/yr STP) per m^2 of seafloor. Aqueous flow velocities, V_{aq}, at the sediment-ocean interface peak at 1.7 to 1.9 cm/yr.

Cumulative Release

Cumulative methane fluxes at the seafloor, C_M, are shown in Figure 3. For the largest temperature change, 5 °C, approximately 1020 mol (23 m^3 STP) of gaseous and dissolved methane escapes per m^2 of seafloor in Case II, while for a 1 °C change, a total of 620 mol (14 m^3 STP) is discharged. Case I, in contrast, discharges 150 to 220 mol (3.4 to 4.9 m^3 STP) per m^2 for 1 °C to 5 °C temperature increases.

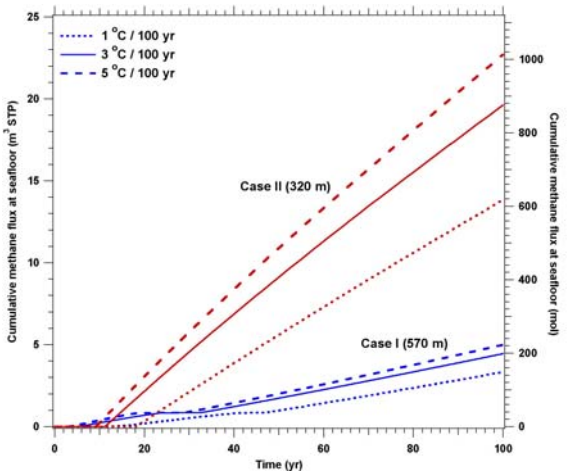

Figure 3: Cumulative methane release, C_M, per m^2 of seafloor for Case I and Case II undergoing 1, 3, and 5 °C increases.

Note that in each of these cases, additional methane gas remains in the sediment column at t = 100 yr (and in Case II, considerable undissociated solid methane hydrate remains as well), therefore release will continue past 100 yr, and cumulative methane generated over longer times is expected to be larger. Extrapolating temperature change scenarios past 100 yr, however, could be regarded as highly speculative, and therefore these simulations are restricted to 100 yr. For any foreseeable continuing temperature-change scenario, hydrate that remains at the end of the simulated time in Case II is unlikely to remain undissociated, and the released gas is unlikely to remain entirely entrained within the sediments.

Chemistry and mitigation of methane release

To provide a first estimate of the response of benthic biochemical communities to sudden releases of methane, we use C.CANDI [22] to model chemistry within the upper 1 m of the sediment column. Detailed data on the nature and chemical composition of benthic sediments above HBS are lacking, however, in several detailed studies of Hydrate Ridge (Cascadia Margin, ODP 204) cold-vent sites [24, 25], Luff and collaborators used data from sediment coring to establish seafloor and bottom-water boundary values and estimate kinetic rate constants for AOM and carbonate precipitation. As this is the most detailed study to date involving hydrate systems near the seafloor with established benthic biological communities, this work uses it as a starting point for our preliminary investigation.

Our simulations model the top 1 m of the sediment column using 1,050 gridblocks, with $\Delta z = 5\text{x}10^{-4}$ m near the seafloor ($z > -0.05$ m), to resolve steep concentration gradients, expanding to $\Delta z = 1\text{x}10^{-3}$ m. The top boundary conditions, representing concentrations of SO_4^{2-}, Ca^{2+}, other trace species, and pH for the overlying seawater, are taken from [25], along with measured and estimated kinetic rate constants derived from the Hydrate Ridge system. As we are interested in short timeframes ($t <$ 100 yr), we disregard sedimentation and organic matter flux to the seafloor. Bioturbation coefficients are set to moderate values [25] representing an active benthic community as seen in deep-sea submersible explorations of Gulf of Mexico hydrate deposits [19]. The effect of carbonate precipitation on porosity and fluid flow is recognized [24]. The lower boundary of the system is modeled with the application of a fixed aqueous fluid velocity, V_{aq}, and an aqueous methane concentration, X_M, derived from the simulations performed in Case I and Case II, along with mineral concentrations reflecting deep pore water data from the Hydrate Ridge system [24]. These bottom-waters are anoxic, and any oxidation of methane will be through AOM processes.

Case I: The release of methane at the seafloor in Case I exhibits two peaks, a first release of methane in the aqueous phase ($Q_{M,aq}$ = 2.2 mol/yr/m^2 for ΔT = 3ºC with V_{aq} = 6.3 cm/yr) begins at t = 4 yr, followed by a drop in $Q_{M,aq}$ at t = 24 yr, with a subsequent release in the gas phase beginning at t = 32 yr. V_{aq} is near zero during this second phase of methane release, reflecting gas movement through buoyancy without strong pressure gradients and fluid advection in the sediment column. Therefore, we model the chemical response of the topmost 1 m of the 1-D sediment column for Δt = 20 yr, using a constant V_{aq} = 6.3 cm/yr and an aqueous methane concentration of X_M = 34.9 mM (0.559 kg/m^3), matching the average for the released aqueous phase in Case I at t = 4-20 yr. The C.CANDI code does not account for multiple phases, therefore we are restricted to chemistry within the aqueous phase, assuming that methane transported as gas escapes AOM.

After 20 years of methane release a significant quantity of the aqueous methane has been oxidized. Of the Q_M = 2.2 mol/yr/m^2 flux entering the reactive zone, only 0.046 mol/yr/m^2 escapes at the seafloor. A flux of 0.52 mol/yr/m^2 CO_2 also escapes at the seafloor, with the remaining methane-derived carbon transported as aqueous HCO_3^- and precipitating, at equilibrium, with Ca^{2+} as solid carbonates. A downward SO_4^{2-} flux of 2.1 mol/m^3/yr into the seafloor drives methane oxidation in the anoxic benthic environment. The system exhibits a total vertically integrated AOM rate of 1.69 mol/yr/m^2. Of the C_M = 40 mol/m^3 of methane released cumulatively between t = 0 and t = 24 yr (Figure 3), less than 2% may actually reach the water column—however, we assume that a significant portion of the subsequent 160 mol/m^3 of gaseous methane ($t >$ 32 yr) will not participate in AOM processes and may escape the seafloor.

Profiles of sulfate and methane concentrations, X_M, after Δt = 20 yr are shown in Figure 4. Sulfate (red line) from the overlying ocean diffuses downward, meeting advecting aqueous methane (blue line) moving upward, forming a "sulfate exclusion zone" to approximately z = -0.1 m. Near the crossing point between sulfate and methane concentrations, the AOM product of HCO_3^- combines with Ca^{2+} to precipitate authigenic carbonate. The carbonate layer is less than 20 cm thick after 20 years, contains less than 1.5 wt% carbonate, and does not affect porosity (and therefore fluid fluid) significantly. Thick carbonate crusts studied in situ typically require centuries to form [25], and therefore it is not surprising that sequestration in the solid phase is not significant on short timescales.

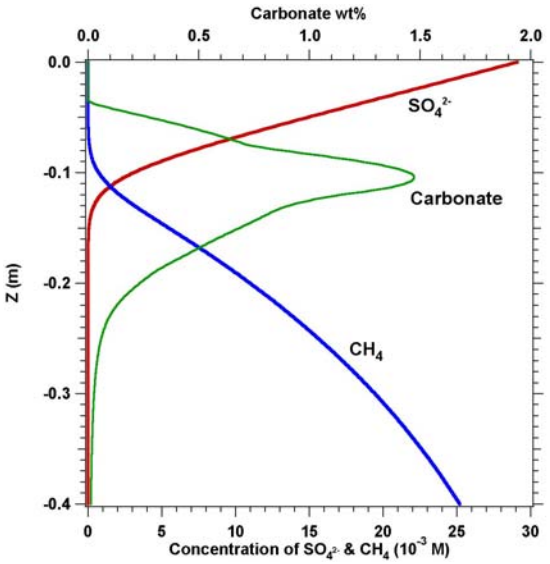

Figure 4: Concentration of sulfate and methane, and wt% carbonates after 20 yr of aqueous methane flux in Case I.

Case II: Methane release at the seafloor in Case II begins abruptly at t = 11 yr and continues at a relatively constant rate until the end of the simulation at t = 100 yr. For this period, Δt = 89 yr, the average V_{aq} = 2.5 cm/yr and the average aqueous flux $Q_{M,aq}$ = 1.35 mol/yr/m^2 (compared to a total average Q_M ~ 10 mol/yr/m^2 in both phases, as methane flux is largely in the gas phase for Case II) corresponding to an average aqueous methane concentration of 54.4 mM (0.871 kg/m^3). However, little is known about possible chemosynthetic communities along the arctic continental shelf. Although the arctic is very biologically active, it also seems likely that AOM rates, if significant at all, would be significantly reduced. Using the existing set of reaction rates at lower temperatures should provide an upper limit to the possible mitigation of methane release by AOM.

After 89 yr of methane release for Case II, again we see significant consumption of aqueous methane under the assumption of an establish, active biological community. Of the $Q_{M,aq}$ = 1.35 mol/yr/m^2 entering the reactive zone, effectively no methane exits at the seafloor. A SO_4^{2-} flux of 1.2 mol/yr/m^2 drives AOM processes, producing 0.09 mol/yr/m^2 CO_2 with the rest of the methane-derived carbon oxidized to bicarbonate or precipitating as solid carbonate. Vertically integrated AOM rates reach 1.20 mol/yr/m^2 after Δt = 89 yr. However, even considering this upper limit to methane consumption, over 85% of the methane release at the seafloor is in the gas phase, not considered in this calculation, and likely to escape mitigation by AOM.

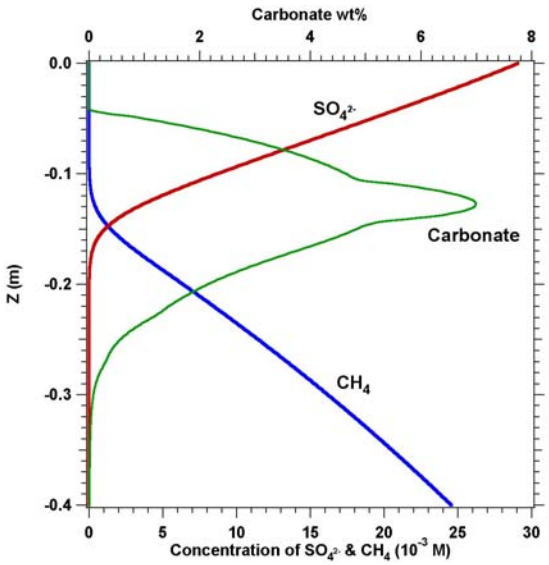

Figure 5: Concentration of sulfate and methane, and wt% carbonates after 89 yr of aqueous methane flux in Case II.

Figure 5 shows profiles of sulfate (red), methane (blue), and solid carbonate (green) after Δt = 89 yr. With a lower V_{aq} and $Q_{M,aq}$ vs. Case I, the sulfate exclusion zone extends to z = -0.14 m, and a thicker ~25 cm carbonate layer with 7 wt% carbonate resides from z = -0.04 m to z = -0.30 m. The thicker, deeper carbonate layer demonstrates the potential for sequestration of release carbon in the solid phase when conditions promote precipitation. However, extensive, highly saturated carbonate crusts may also reduce sediment porosity and impact vertical fluid flow [25], which may "cut off" crust formation in the vertical direction and disrupt the AOM-driven sequestration processes.

CONCLUSIONS

To determine the fate of oceanic gas hydrate deposits impacted by climate-change induced ocean temperature increases, we performed 1-D multiphase thermodynamic-hydrological modeling of two representative hydrate accumulations, assessing the potential for methane release into the

environment. The analysis considered the properties of benthic sediments, the saturation and distribution of the hydrates, the ocean depth, the initial seafloor temperature and possible temperature change, and for the first time, estimated the effect of benthic biogeochemical activity. The results show that shallow deposits, such as those found in arctic regions or in the Gulf of Mexico, can undergo rapid dissociation under the influence of as little as $1^{o}C$ of seafloor temperature increase. Such dissociation of hydrates can produce significant methane fluxes of up to 13 mol/yr/m^2 (for arctic deposits) over a period of decades, and can release up to 1,100 mol of methane per m^2 of seafloor in a century. The results suggest that rapid release of methane is possible for shallow hydrates in both warm and cold regions, and that arctic hydrates, if found to be as widespread as some evidence suggests, may present a particular threat to regional and global ecology.

These fluxes may exceed the ability of the seafloor environment (via anaerobic oxidation of methane) to consume the released methane or sequester the carbon. Using reaction rate parameters and pore water data measured directly from a hydrate-fueled cold vent site, we estimated AOM mitigation of methane release in the aqueous phase. Although the calculations suggest a strong potential for methane oxidation under the simulated conditions, large-scale sequestration of methane-derived carbon as carbonates is unlikely on a decadal or century timescale. In addition, a large portion of the methane released in the simulated scenarios emerges in the gas phase, possibly reducing the potential for AOM. Fully coupled multiphase flow, transport, and chemistry simulations are needed to develop a complete understanding of the interaction between rapid methane release and the ocean environment, and additional study of arctic hydrate deposits and the surrounding biochemical communities is critical in understanding the potential for regional and global ecological impacts.

ACKNOWLEDGEMENTS

This research has been supported by the Laboratory Directed Research and Development (LDRD) program at Lawrence Berkeley National Laboratory, by the Director, Office of Science, of the U.S. Department of Energy (DoE) under Contract No. DE-AC02-05CH11231, and by the Assistant Secretary for Fossil Energy, Office of Natural Gas and Petroleum Technology, through the National Energy Technology Laboratory (NETL).

REFERENCES

[1] Sloan, E.D. Clathrate Hydrates of Natural Gases, New York:Marcel Decker, Inc., 1998.

[2] Milkov, A.V. *Global estimates of hydrate-bound gas in marine sediments: how much is really out there?* Earth Science Reviews 2004: 66: 183.

[3] Dobrynin, V.M., Korotajev, Y.P., and Plyuschev, D.V. in Long-Term Energy Resources, R. F. Meyer and J. C. Olson, Eds., Boston, MA: Pitman, 1981.

[4] Gornitz V., and Fung, I. *Potential distribution of methane hydrate in the world's oceans.* Global Biogeochem. Cycles 1994: 8: 335.

[5] Holbrook, W.S., Hoskins, H., Wood, W.T., Stephen, R.A., and Lizarralde, D. *Methane hydrate and free gas on the Blake Ridge from vertical seismic profiling.* Science 1996: 273: 1840.

[6] Kvenvolden, K.A. *Potential effects of gas hydrate on human welfare.* Proc. Nat. Acad. Sci. 1999: 96: 3420.

[7] Borowski, W.S. *A review of methane and gas hydrates in the dynamic, stratified system of the Blake Ridge region*, offshore southeastern North America. Chem. Geology 2004: 205: 311.

[8] Klauda, J.B., and Sandler, S.I. *Global distribution of methane hydrate in ocean sediment.* Energy and Fuels: 2005: 19: 459.

[9] Buffett, B., and Archer, D. *Global inventory of methane clathrate: Sensitivity to changes in environmental conditions.* Earth Planetary Sci. Lett. 2004: 227: 185.

[10] Moridis, G.J., and Kowalsky, M.B. *Gas Production from Unconfined Class 2 Hydrate Accumulations in the Oceanic Subsurface,* in Economic Geology of Natural Gas Hydrates, M. Max, A.H. Johnson, W.P. Dillon, and T. Collett, Editors, Kluwer Academic/Plenum Publishers, 2005.

[11] Collett, T.S., and Kuuskraa, V.A. Oil and Gas Journal 1998: 96(19): 90.

[12] Archer, D. *Methane hydrate stability and anthropogenic climate change*, Biogeosciences 2007: 4: 521.

[13] Kennett, J.P., Cannariato, K.G., Hendy, L.L., and Behl, R.J. *Carbon isotopic evidence for methane hydrate instability during quaternary interstadials.* Science 2000: 288: 128.

[14] Hovland, M., Svensen, H., Forsberg, C.F., Johansen, H., Fichler, C., Fossa, J.H., Jonsson, R., and Rueslatten, H. *Complex pockmarks with carbonate-ridges off mid-Norway: Products of sediment degassing.* Marine Geology 2005: 218: 191.

[15] Dickens, G.R., O'Neil, J.R., Rea, D.K., and Owens, R.M. *Dissociation of oceanic methane hydrate as a cause of the carbon isotope excursion at the end of the Paleocene.* Paleoceanography 1995: 10: 965.

[16] Archer, D., and Buffett, B. *Time-dependent response of the global ocean clathrate reservoir to climatic and anthropogenic forcing.* Geochem. Geophys. Geosys. 2005: 6(3): Q03002, doi:10.1029/2004GC000854.

[17] Reagan, M.T. and Moridis, G.J. *Oceanic gas hydrate instability and dissociation under climate change scenarios,* Geophys. Res. Lett. 2007: 34: L22709, doi: 10.1029/ 2007GL031671.

[18] Xu, W., and Lowell, R.P. *Effect of seafloor temperature and pressure variations on methane flux from a gas hydrate layer: Comparison between current and late Paleocene climate conditions.* J. Geophys. Res. 2001: 106(B11): 26413.

[19] Sassen, R., Joye, S., Sweet, S.T., DeFreitas, D.A., Milkov, A.V., and MacDonald, I.R. *Thermogenic gas hydrates and hydrocarbon gases in complex chemosynthetic communities, Gulf of Mexico continental slope.* Organic Geochemistry 1999: 30: 485.

[20] Boetius, A., and Suess. *E. Hydrate Ridge: a natural laboratory for the study of microbial life fueled by methane from near-surface gas hydrates*. Chemical Geology 2004: 205: 291.

[21] Boudreau, B.P., Computers and Geosciences 1996: 22(5): 479.

[22] Luff, R., Wallmann, K., Grandel, S., and Schluter, M., Deep-Sea Research II 2000: 47: 3039.

[23] Luff, R., and Wallmann, K., Geochim. Cosmochim. Acta, 2003: 67(18): 3403.

[24] Luff, R., Greinert, J., Wallmann, K., Klaucke, I., and Suess, E., Chemical Geology 2005: 216: 157.

[25] Luff, R., Wallmann, K., and Aloisi, G., Earth and Planetary Sci. Lett. 2004: 221: 337.

[26] Valentine, D.L., Blanton, D.C., Reeburgh, W.S., and Kastner, M., Geochim. Cosmochim. Acta 2001: 65(16): 2633.

[27] Brewer, P.G., Paull, C., Peltzer, E.T., Ussler, W., Rehder, G., and Friederich, G., Geophys. Res. Lett. 2002: 29(22): 2081.

[28] Moridis, G.J., Kowalsky, M.B., and Pruess, K., TOUGH-Fx/HYDRATE v1.0 User's Manual. Report LBNL-58950, Lawrence Berkeley National Laboratory, Berkeley, CA, 2005.

[29] Moridis, G.J. *Numerical studies of gas production from methane hydrates*, SPE-87330, SPE Journal 2003: 359.

[30] Tang, L-G, Li, X-S, Feng, Z-P, Li, G., and Fan, S-S. *Control mechanisms for gas hydrate production by depressurization in different scale hydrate reservoirs*. Energy & Fuels 2007: 21: 227.

[31] Moridis, G.J., Collett, T.S., Dallimore, S.R., Inoue, T., and Mroz, T. *Analysis and Interpretation of the Thermal Test of Gas Hydrate Dissociation in the JAPEX/JNOC/GSC et al. Mallik 5L-38 Gas Hydrate Production Research Well*, in Geological Survey of Canada, Bulletin: 585: S.R. Dallimore and T. Collett, Eds, 2005.

[32] Moridis G.J. and Sloan, E.D. *Gas production potential of disperse low-saturation hydrate accumulations in oceanic sediments*. Energ. Convers. Manag. 2007: 48: 1834.

[33] Milkov, A.V., and Sassen, R. *Estimate of gas hydrate resource, northwestern Gulf of Mexico continental slope.* Marine Geology 2001: 179: 71.

[34] Ginsburg, G.D. and Soloviev, VA. Submarine Gas Hydrates. St. Petersburg, 1998.

[35] Spinelli, G.A., Giambalvo, E.R., and Fisher, A.T. *Sediment permeability, distribution, and influence on fluxes in oceanic basement.* Hydrogeology of the Oceanic Lithosphere, E.E. Davis and H Elderfield, Eds. Cambridge University Press, 2004.

[36] CCSM Special Overview Issue, Journal of Climate 2006: 19: 11.

[37] Moridis, G.J., Seol, Y., Kneafsey, T. *Studies of reaction kinetics of methane hydrate dissociation in porous media* (Paper 1004), Proceedings of the 5th International Conference on Gas Hydrates, Trondheim, Norway, 12-16 June 2005.

[38] Van Genuchten, M.T. *A closed-form equation for predicting the hydraulic conductivity of unsaturated soils*, Soil Sci. Soc. 1980: 44: 892.

[39] Stone, H.L. *Probability model for estimating three-phase relative permeability.* Trans. SPE AIME 1970: 249: 214.